International Journal of Recent Technology and Engineering (IJRTE)
ISSN: 2277-3878 (Online), Volume-9 Issue-3 September 2020

Implementation of Iterative bilateral filtering for removal of Rician noise in MR images using FPGA

Durga Pathrikar, V. N. Jirafe

Abstract: ***Magnetic resonance image noise reduction is important to process further and visual analysis. Bilateral filter is denoises image and also preserves edge. It proposes Iterative bilateral filter which reduces Rician noise in the magnitude magnetic resonance images and retains the fine structures, edges and it also reduces the bias caused by Rician noise. The visual and diagnostic quality of the image is retained. The quantitative analysis is based on analysis of standard quality metrics parameters like peak signal-to-noise ratio and mean structural similarity index matrix reveals that these methods yields better results than the other proposed denoising methods for MRI. Problem associated with the method is that it is computationally complex hence time consuming. It is not recommended for real time applications. To use in real time application a parallel implantation of the same using FPGA is proposed.***

Keywords: Iterative Bilateral Filtering, MRI, Rician Noise, FPGA

I. INTRODUCTION

Magnetic images are corrupted by several artifacts and noise sources. The patient's body is conductive medium and can generate fluctuating field which can be picked up receiver as a noise. Noise in MRI impacts visual analysis and diagnosis. For accurate diagnosis, image quality can be improved using image denoising. Earlier assumption was that noise in the MRI as Gaussian, which does not take into account biasing effect which is caused by Rician noise and MR images noise can be characterized by Rician distribution. There were some methods proposed for denoising MR images are the non-local means (NLM)[6], partial differential equations (PDE)[6], wavelets and maximum likelihood (ML)[6] estimation methods. NLM based methods were proposed for denoising magnitude MR images. Bilateral filter is nonlinear filter which is combination of range and domain filters is accurate and which blurs image but restores fine structures and edges and iterative Bilateral filter which improves denoising efficiency but requires more computation. To reduce computation time FPGA can be used, which employs parallelism and dedicated custom hardware to reduce processing time.

A. Noise characteristics in MRI:

The major source of noise in MRI is thermal in origin which is result of the stochastic motion of free electrons[6].

Revised Manuscript Received on August 29, 2020.
***** Correspondence Author
Mrs. Durga Pathrikar, Department of Electronics and Telecommunication, PES's Modern College of Engineering, Pune, India. E-mail: Kulkarnidurga14@gmail.com
Prof. Mrs. V. N. Jirafe, Professor, Department of Electronics and Telecommunication, PES's Modern College of Engineering, Pune, India. E-mail: vnjpune@gmail.com

The captured raw complex MR data initially thought to be Gaussian and the presence of thermal noise in the k-space are characterized by a Gaussian probability density function (PDF).

Using Fourier Transform the magnetization distribution is obtained from k-space data. The data distribution in the real and imaginary components is Gaussian and nonlinear. The magnitude of the reconstructed MR image is commonly used to inspect images and for automated computer analysis. Since data is non linear and complex, noise can characterized by Rician distribution.

When PSNR is high, noise is characterized by Gaussian distribution and at low PSNR it is characterized by Rayleigh Distribution.

The probability distribution function (PDF) of the magnitude data will be a Rician distribution,

$$P_{mag}(M)=\frac{M}{\sigma^2}e^{\frac{-M^2+A^2}{2\sigma^2}}I_0\left(\frac{AM}{\sigma^2}\right), \quad M\geq 0 \qquad (1)$$

Where $M=\sqrt{\Re^2+\Im^2}$, $A=\sqrt{\mu_{\Re}^2+\mu_{\Im}^2}$

And I_0 is the modified first of kind Bessel function with order zero.

The first two moments of the Rice PDF becomes,

$$E[M]=\sigma\sqrt{\frac{\Pi}{2}}\ e^{\frac{-A^2}{4\sigma^2}}\left[\left(1+\frac{A^2}{2\sigma^2}\right)I_0\left(\frac{A^2}{4\sigma^2}\right)+\frac{A^2}{2\sigma^2}I_1\left(\frac{A^2}{4\sigma^2}\right)\right] \qquad (2)$$

$$E[M^2]=A^2+2\sigma^2 \qquad (3)$$

The Rician distribution approaches to Rayleigh distribution when the SNR goes to zero.

$$P_{mag}(M)=\frac{M}{\sigma^2}e^{\frac{-M^2}{2\sigma^2}}, \quad M\geq 0 \qquad (4)$$

When SNR is high, the Rician distribution changes to a Gaussian distribution.

$$P_{mag}(M)=\frac{1}{\sqrt{2\Pi\sigma^2}}e^{\frac{-(M-\sqrt{A^2+\sigma^2})^2}{2\sigma^2}} \qquad (5)$$

In an Iterative bilateral filter, two pixels can be close to one another in terms of spatial location or nearby values. Closeness implies to nearby area in the domain, and similarity means nearby area in the range. Traditional filtering uses domain filtering, and closeness is determined by weighing pixel values with coefficients which decreases with distance. Similarly, range filtering uses averaging image values with weights which is ineffective for dissimilarity. Range filters are nonlinear in nature as their weights rely on image intensity.

The product of domain and range filter is called Bilateral filter. Following equation provides the location of pixel x,

$$\hat{I}(x) = \frac{1}{C} \sum_{y \epsilon N(x)} w_s(x,y)\ w_R(x,y)\ I(y) \quad (6)$$

$$w_s(x,y) = \exp\left(\frac{-|x-y|^2}{2\sigma_d^2}\right) \quad (7)$$

The weight function w_s is inversely proportional to spatial distance.

The weight function w_R is inversely proportional to the radiometric distance.

Let M_1 , M_2 , M_3 ,…. M_n be statistically independent observations where signal intensity A is constant. The joint PDF observations is,

$$P(\{M_i\}|A) = \prod_{i=1}^{n} \frac{M_i}{\sigma^2} e^{\frac{-M_i^2 + A^2}{2\sigma^2}} I_0\left(\frac{AM_i}{\sigma^2}\right) \quad (8)$$

In the PDF unknown parameters can be estimated using maximizing the corresponding likelihood function L(A):

$$\text{Ln } L(A) = \sum_{i=1}^{n} \ln\left(\frac{M_i}{\sigma^2}\right) - \sum_{i=1}^{n} \frac{M_i^2 + A^2}{2\sigma^2} + \sum_{i=1}^{n} \ln I_0\left(\frac{AM_i}{\sigma^2}\right) \quad (9)$$

For the noise variance a Robust estimator can be written as the mode of all ML estimated local noise levels as,

$$\hat{\sigma}^2 = mode\left\{\hat{\sigma}^2_{ML(i)}\right\} \quad (10)$$

When dealing with MR images, the bias introduced is due to Rician noise. In this the image data is applied to bilateral filter iteratively after bias reduction. Bias can be reduced by subtracting $2\sigma^2$ from the squared image as it is biased on second moment of the Rician distribution.

$\hat{I}_1$ be the denoised image after first iteration, with bias correction it becomes:

$$\hat{I}_1 = \sqrt{\max\left(\hat{I}_1^2 - 2\hat{\sigma}^2, 0\right)} \quad (11)$$

Bilateral filter is applied iteratively. The noise level σ will reduce after each iteration and it has to be re-estimated after each iteration.

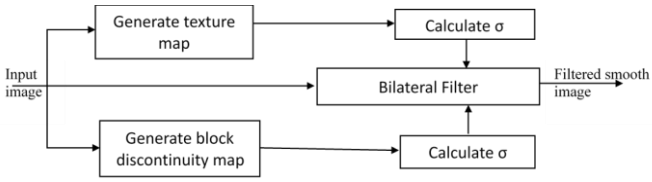

Figure.1 Block diagram of bilateral filter

B. Bilateral Filter:

A bilateral filter is a smoothening filter and it preserve the edges. It consist of two types of filters i.e. Domain filter and Range filter. Input image is feed to generate texture map block to provide domain filter constant to bilateral filter similarly discontinuity map is used to provide range filter constant to bilateral filter.

Noise affects the pixel values in the image which can cause random variation of brightness and color of image. Gaussian noise which gets added in image during acquisition process, it is additive in nature and adds random value to pixel.

Unlike conventional filter Bilateral filter uses both domain as well as range filtering. Range filtering applies to the gray map of the image and it does not have notion of space. Range filtering chooses values based on low pass filtering, domain filters, values chosen based on desired amount of combination filter.

C. Iterative bilateral filter:

- Filters Rician noise in the magnitude magnetic resonance images.
- It reduces bias due to noise and retains the fine structures and blurs image.
- It can be evaluated using standard quality metrics.
- Maximum three iteration Bilateral Filter has been implemented as same will be realized on FPGA in second phase, complexity on FPGA increases with every iteration so 3 iterations have been used for Iterative Bilateral Filter.
- Select image using MATLAB based GUI.
- Breaks image into block of pixels of 4x4 or 8x8
- Transfer block of pixel to FPGA using RS232 protocol.
- Reconfigurable FPGA is performing the task by receiving input pixels and apply Iterative bilateral filter (implemented on FPGA) on it.

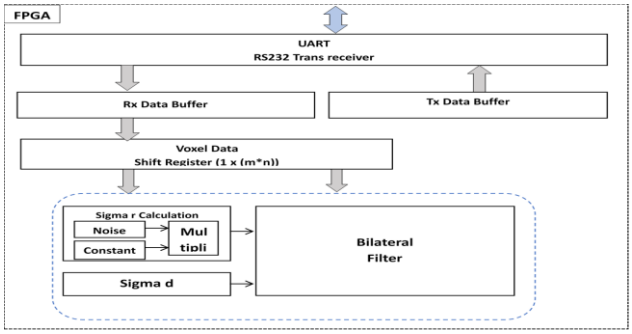

Figure 2. Block diagram of Iterative Bilateral Filter on FPGA

D. Hardware Realization of Iterative Biltaral Filter:

1) FPGA:

FPGA stands for field programmable gate arrays that can be configured by the customer or designer after manufacturing., they are structured very much like a gate array ASIC. FPGAs are programmed using a logic circuit diagram or using hardware description language (HDL) which specifies chip function.

II. HARDWARE SPECIFICATIONS:

A. SPARTAN 6 FPGA

Mimas spartan 6 FPGA Development board is based on Xilinx Spartan-6 FPGA. Xilinx Mimas board is development kit for system designer. It has Xilinx XC6SLX9 TQG144 FPGA. The USB 2.0 communication interface, on-board SPI flash for configuration.

1) SPARTAN 6 FPGA Features

• FPGA: Spartan XC6SLX9 in TQG144 package is development board has 16 Mb SPI flash memory (M25P16), usb interface for On-board flash programming,

FPGA configuration via JTAG and USB, user configurable 70 IOs

III. SOFTWARE SPECIFICATIONS:

A. MATLAB 2020a:

MATLAB used as software development tool for Filter development which includes GUI and .

IV. ADVANTAGES AND APPLICATIONS OF BF AND IBF:

A. Advantages:

- Iterative Bilateral filter improves denoising efficiency.
- Smoothen an image while preserving its discontinuities
- Preserves fine structures, edges and reduces bias.

B. Applications:

- MR images
- Image processing

Results of MRI for different noise levels:

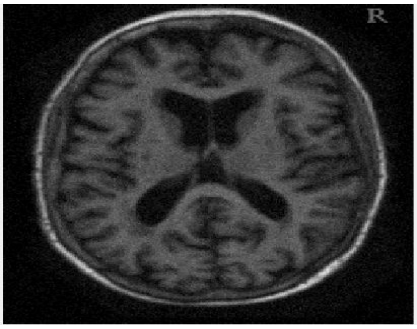

Figure 3 [a]. Noisy Input Image

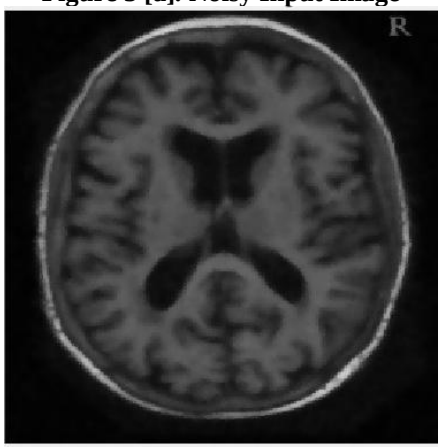

Figure 3 [c] Denoised output of BF

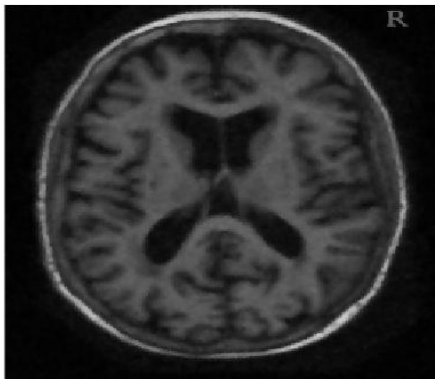

Figure 3 [b] Denoised output of IBF

Table 1:T1 Weighted Brain Scan MR Image (I) BF/IBF Filter Result

Image 1 (BF and IBF) filter parameter evaluation											
	Noise	10	15	20	25	30	35	40	45	50	55
PSNR	BF	20.4327	18.038	16.0657	14.5026	13.1084	11.9982	11.0274	10.1345	9.3939	8.7102
	IBF	19.391	20.155	19.7291	17.4062	15.9543	14.5501	12.6106	11.9003	10.7029	9.5051
SSIM	BF	0.75939	0.66514	0.54009	0.42401	0.32393	0.2494	0.1988	0.1566	0.1268	0.1057
	IBF	0.7483	0.75995	0.75494	0.70276	0.66839	0.6345	0.5965	0.5729	0.5482	0.5108
PRAT	BF	96.514	95.7039	93.3308	83.834	74.5402	69.676	63.7679	59.6055	60.4188	62.9631
	IBF	97.1459	96.1429	92.66	91.4057	90.2987	86.4292	82.4542	82.4091	77.4174	79.4228
CORRELATION	BF	0.98878	0.97535	0.94715	0.90162	0.83399	0.7606	0.6811	0.6029	0.5272	0.4613
	IBF	0.9824	0.98028	0.97532	0.96498	0.95168	0.9404	0.9284	0.9107	0.8971	0.8785

Table 2: Comparison of average Time required to process voxel on computer

Sr. No.	BF	IBF
1	218.0 ms	289.3 ms

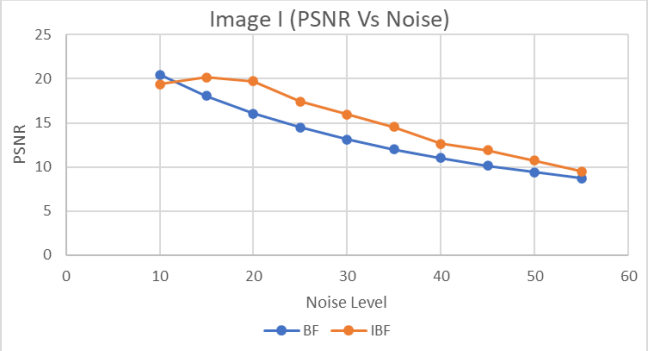

Figure 4 [a] Graph: PSNR Vs Noise Level (Image I)

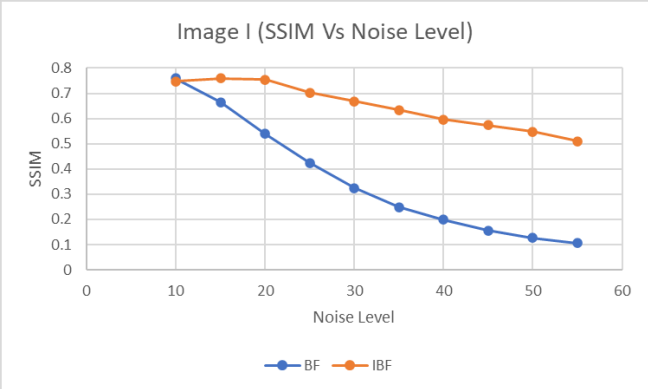

Figure 4 [b] Graph: SSIM Vs Noise Level (Image I)

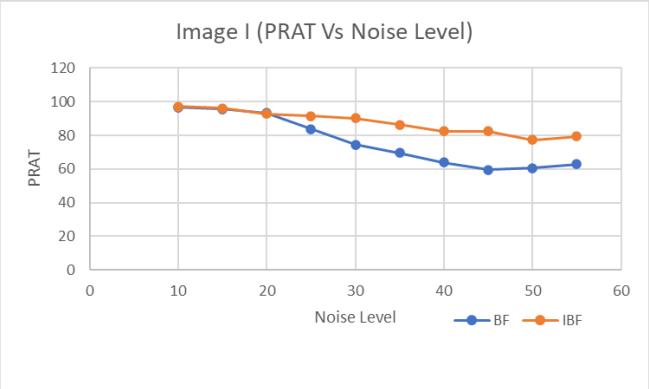

Figure 4 [c] Graph: SSIM Vs Noise Level (Image I)

Table 3:T1 weighted brain scan MR Image (I) BF/IBF

Image II (BF and IBF) filter parameter evaluation											
	Noise	10	15	20	25	30	35	40	45	50	55
PSNR	**BF**	20.1649	17.7513	15.875	14.31	12.9426	11.8711	10.8749	10.045	9.2844	8.5972
	IBF	19.1206	18.4548	16.099	15.1649	12.5004	11.5246	9.7186	9.0203	9.0115	7.6119
SSIM	**BF**	0.73418	0.63415	0.51599	0.40368	0.30726	0.23961	0.18948	0.15045	0.12154	0.098741
	IBF	0.74231	0.74768	0.67608	0.62916	0.57471	0.54912	0.50056	0.4801	0.47299	0.43136
PRAT	**BF**	96.7672	93.6507	85.5807	79.3093	69.0675	62.6509	59.2523	59.92	62.0148	59.9525
	IBF	97.4136	96.6237	94.7132	93.7386	89.9339	88.0417	83.5546	78.7964	82.8519	75.5169
CORRELATION	**BF**	0.98894	0.97492	0.94621	0.89936	0.82907	0.75341	0.66943	0.59179	0.51745	0.44884
	IBF	0.9854	0.98184	0.97374	0.96258	0.95508	0.94466	0.93258	0.92234	0.90167	0.89012

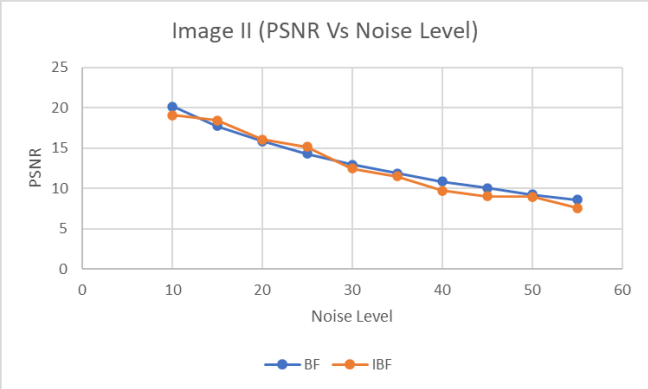

Figure 5 [a] Graph: PSNR Vs Noise Level (Image II)

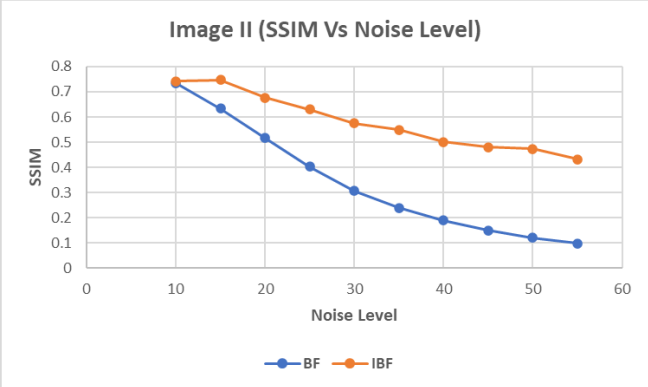

Figure 5 [b] Graph: SSIM Vs Noise Level (Image II)

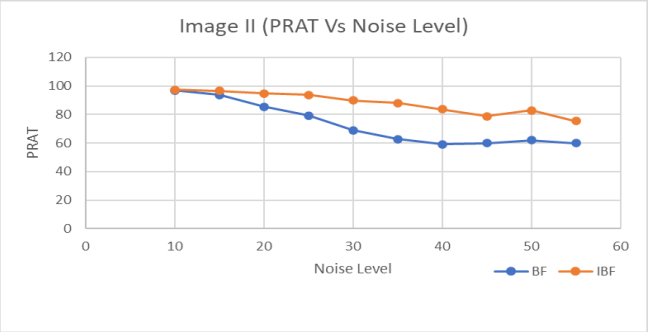

Figure 5 [c] Graph: PRAT Vs Noise Level (Image II)

C. Result for Iterative Bilateral Filter on FPGA:

Table 4: Processing time optimization on FPGA:

Device Utilization Summary (Estimated Value)			
Logic Utilization	**Used**	**Available**	**Utilization**
No. of slice LUTs	1242	5720	21%
No. of fully used LUT-FFT pair	0	1242	0%
No. of bonded IOBs	50	102	49%
No. of DSP48A 1s	6	16	37%

Table 5: FPGA Device Utilization Summary:

Parameters	Time/Frequency
Min. Period	14.540 MHz
Min. i/p arrival time before clock	2.021 ns
Max. o/p required time after clock	3.597 ns
Max. Combination path delay	81.435 ns

FPGA and MATLAB Look Up Table Comparison:
Gaussian Distance weights Lookup table

A. MATLAB Lookup table

Table 6: Pre-computed Gaussian Distance weights in matlab with inputs, window size 3x3, sigma_d=1.8

0.107	0.1131	0.107
0.1131	0.1196	0.1131
0.107	0.1131	0.107

Table 7: Scaled by 100, Pre-computed Gaussian Distance VHDL Lookup table:

10.7	11.31	10.7
11.31	11.96	11.31
10.7	11.31	10.7

Table 8: Lookup table implemented in VHDL by rounded scaling with 100

10	11	10
11	11	11
10	11	10

Negative Exponential Lookup table

B. Matlab Lookup table

Table 9: Pre-computed negative exponential lookup table in Matlab (input 0 to 10)

0	1	2	3	4	5	6	7	8	9	10
1	0.3679	0.1353	0.0498	0.0183	0.0067	0.0025	0.0009	0.0003	0.0001	0

Table 10: Scaled by 100

0	1	2	3	4	5	6	7	8	9	10
1	36.79	13.53	4.98	1.83	0.67	0.25	0.09	0.01	0.01	0

C. VHDL Lookup table:

Table 11: Lookup table implemented in vhdl by rounded scaling with 100

0	1	2	3	4	5	6	7	8	9	10
100	36	13	4	1	0	0	0	0	0	0

Approximation Error

Table 12: Error between theoretical lookup table values and implemented VHDL lookup table:

0	1	2	3	4	5	6	7	8	9	10
0	0.79	0.53	0.98	0.83	0.67	0.25	0.09	0.01	0.01	0

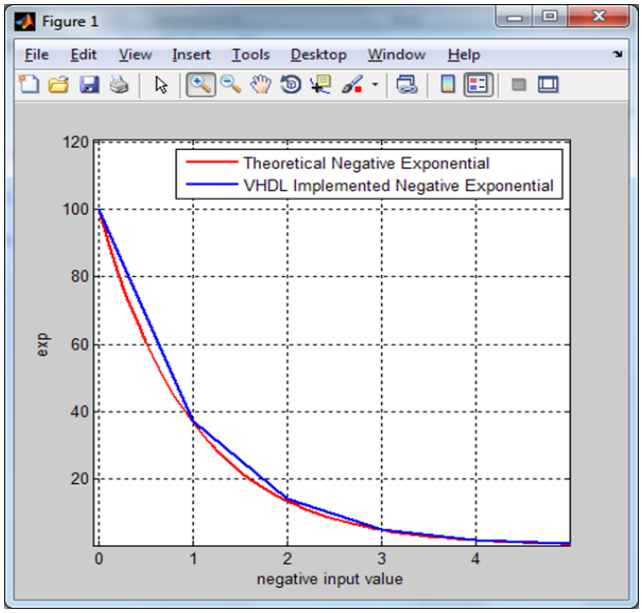

Figure 6 Graph: Negative Exponential Comparison Gap

V. DISCUSSION:

For quantitative analysis of denoising methods, various parameters like peak signal-to-noise ratio (PSNR), SSIM, PRAT and correlation has been evaluated.

A. PSNR:

It is peak signal to noise ratio. The high PSNR value indicates good quality of the compressed or reconstructed image.

$$PSNR = 10\log_{10}\left(\frac{R^2}{MSE}\right) \quad (12)$$

For comparative analysis experiments were conducted with various real MR images and these images artificially corrupted by adding noise and tested with Bilateral and Iterative Bilateral Filter and PSNR and MSE computed of denoised image.

As from result, it clearly shows that with iterative Bilateral Filter, PSNR,SSIM and PRAT has improved.

Iterative Bilateral Filter improves the quality of MR images and help in preserving fine structures and edges in the MR images.

From Visual analysis it is observed that the denoised MR images gives much better result in terms of image contrast image and restoration.

IBF have been implemented and evaluated on computer using MATLAB and on FPGA, later gives considerable improvements in terms of time.

VI. CONCLUSION

A. Quality Metrics: Improvements in an iterative bilateral filter over a bilateral filter have been assessed by quality metrics parameters SSIM and PRAT, which found on an average 38.18% and 2.68% respectively.

B. Computation Time: BF takes about on an average 218 ms to process one voxel and IBF takes about on an average 289 ms, so IBF is computationally more complex and requires more time,

C. Time Improvement using FPGA: From FPGA prototype development and test, it is evident that computation time has reduced drastically from 200+ ms to 100+ ns to process voxel if we consider average time.

REFERENCES

1. Wright, G.: Magnetic resonance imaging. IEEE Signal Process. Mag. 1, 56–66 (1997)
2. Nishimura, D.G.: Principles of Magnetic Resonance Imaging. Stanford University, Stanford, CA (2010)
3. Manjón, J.V., Carbonell-Caballero, J., Lull, J.J., Garciá-Martí, G., Martí-Bonmatí, L., Robles, M.: MRI denoising using non-local means. Med. Image Anal. **12**, 514–523 (2008)
4. Wiest-Daesslé, N., Prima, S., Coupé, P., Morrissey, S. P., Barillo, C.: Rician noise removal by non-local means filtering for low signal-to-noise ratio MRI: applications to DT-MRI. In: Proceedings of MICCAI, pp. 171-179 (2008)
5. Manjón, J.V., Coupé, P., Martí-Bonmatí, L., Collins, D.L., Robles, M.: Adaptive non local means denoising of MR images with spatially varying noise levels. J. Magn. Reson. Imaging **31**, 192–203(2010)
6. R. Riji, Jeny Rajan, Jan Sijbers, Madhu S. Nair. "Iterative bilateral filter for Rician noise reduction in MR images", Signal, Image and Video Processing, 2014

AUTHORS PROFILE

Durga Pathrikar, student of M.E. Signal processing, P. E. S.'s Modern college of Engineering affiliated to SPPU Pune.